Calculation of energy levels and polarized oscillator strengths for Nd^{3+}:YAG

Mattias Klintenberg, Sverker Edvardsson,* and John O. Thomas
Ångström Laboratory, Uppsala University, Inorganic Chemistry, Box 538, S-751 21 Uppsala, Sweden
(Received 7 October 1996)

The effect of an electrostatic crystal-field (CF) model on energy levels and oscillator strengths for Nd^{3+}:YAG (where YAG denotes yttrium aluminum garnet) has been studied. Three parameters for the correction of the Slater integrals F^2, F^4, and F^6 and one parameter to correct the spin-orbit constant for the effects of the linear configuration interaction have been introduced. The complete 364×364 energy matrix has been diagonalized directly. The various polarizabilities and shielding parameters used have been calculated by *ab initio* methods. All Stark levels within the $Nd^{3+}(4f^3)$ configuration are presented. The calculated Stark splittings agree well with experiment. The electrostatic CF model used is therefore believed to be satisfactory. The eigenvectors of the complete energy matrix have been used to calculate oscillator strengths, which agree well with experiment. A refined Judd-Ofelt theory has been used. The Judd-Ofelt intensity parameters Ω_λ are presented and found to be in excellent agreement with experiment. The temperature dependence of the spectrum is studied using a molecular-dynamics approach. [S0163-1829(97)07316-5]

I. INTRODUCTION

The analysis of complex absorption spectra of the rare-earth elements is usually based on parameters derived by least-squares fitting to experiment. Using the powerful operator techniques developed by Racah[1–4] and a good set of radial functions, it is possible to greatly reduce the number of parameters, usually more than 30. In this work, the assumption is made that we have a pure $4f^3$ configuration, i.e., the configuration interaction (CI) is not included.[5] A complete CI calculation will remove all four parameters c_2, c_4, c_6, and c_ζ, introduced into our calculation. The Hamiltonian used is the standard $H=H_0+H_{\rm EL}+H_{\rm SO}+H_{\rm CF}$. The electrostatic crystal field used in $H_{\rm CF}$ is calculated for each individual environment by direct summation over the rare-earth ion environment until convergence is achieved. Each ion in the environment is multipole expanded; different polarizabilities as well as the shielding parameters have been derived from *ab initio* methods.[6] More sophisticated crystal-field (CF) models can be used,[7–12] but have a negligible effect compared to that resulting from our molecular-dynamics (MD) treatment, at least in this case. An electrostatic model here gives a quite satisfactory result. The radial wave functions needed for all radial integrals are evaluated using the Hartree-Fock-Dirac approximation.[6] Once the energy matrix is obtained, it can be diagonalized to yield the eigenvalues and eigenvectors. The polarized oscillator strengths are computed, although Nd^{3+}:YAG (where YAG denotes yttrium aluminum garnet) is optically isotropic, using a refinement of Judd-Ofelt theory. Only electric-dipole transitions are considered within the $4f$ shell. In this way, a polarized absorption or emission spectrum can be generated at different temperatures. In an absorption spectrum, the ground-state levels are assumed to have a Boltzmann population. When the temperature is raised, the motion of the ions becomes nonnegligible and must be taken into account. This is done using MD simulation. MD generates different physical environments, implying that the Stark levels and the oscillator strengths must be calculated for each environment and an appropriate histogram constructed. All programs used have been implemented within our group.

II. THEORY

A. Matrix elements

Using Racah algebra[1–4] and the fact that $H_0\gg H_{\rm EL}\gg H_{\rm SO}\gg H_{\rm CF}$ in $H=H_0+H_{\rm EL}+H_{\rm SO}+H_{\rm CF}$, the matrix elements of the different Hamiltonians can be expressed in more manageable forms. We use atomic units and the number of electrons is 3 throughout the calculations. The fractional parentage coefficients appearing in the formulas below can be calculated using Eqs. (34), (52a), (52b), and (56) and Tables IIIa and IVa in Racah's fourth classic paper.[4] For the case of f^3, the coefficients are tabulated in Table 1 of Ref. 13. Quantum numbers belonging to the parent state are barred.

$H_{\rm EL}$ is given by the standard expression

$$H_{\rm EL}=\frac{1}{2}\sum_{i\neq j=1}^{3}\frac{1}{|r_i-r_j|}=\frac{1}{2}\sum_{\substack{t=0\\ i\neq j}}^{\infty}\frac{r_<^t}{r_>^{t+1}}\,C_{tp}^*(\hat{\mathbf{r}}_i)C_{tp}(\hat{\mathbf{r}}_j). \tag{1}$$

The matrix element for $H_{\rm EL}$ becomes[13]

$$\begin{aligned}\langle \gamma SL|H_{\rm EL}|\gamma' S'L'\rangle=\frac{1}{2}\sum_{t=2,4,6}c_tF^t\Bigg(&3\delta_{\gamma'\gamma}(2l+1)^{-1}\\&+6\sum_{\bar{L}}(-1)^{\bar{L}}\langle f^3\gamma SL\{|f^2\overline{SL}\rangle\\&\times\langle f^3\gamma' S'L'\{|f^2\overline{SL}\rangle\\&\times\begin{Bmatrix}l&l&\bar{L}\\l&l&t\end{Bmatrix}\Bigg)|\langle l\|C^t\|l\rangle|^2\delta_{S'S}\delta_{L'L}.\end{aligned} \tag{2}$$

F^t are the Slater integrals given by

TABLE I. Values of radial integrals, shielding, and configuration interaction parameters in a.u.

Integrals	*ab initio*[a]	Phenomenological[b]	σ^t [a]	c_t, c_ζ
$\langle r^2\rangle$	1.222		0.514	
$\langle r^4\rangle$	3.873		0.0164	
$\langle r^6\rangle$	26.032		−0.0307	
$F^{(2)}$	0.457	0.323		0.706
$F^{(4)}$	0.289	0.233		0.808
$F^{(6)}$	0.211	0.158		0.750
ζ	78.97[c]	129.82		1.644

[a]Reference 6.
[b]Reference 22.
[c]Calculated in this work.

$$F^t = 2\int_0^\infty dr\ R_{4f}^2(r)\int_r^\infty dr' R_{4f}^2(r')\ \frac{r^t}{r'^{t+1}}. \tag{3}$$

$H_{\mathrm{SO}} = c_\zeta \zeta \Sigma_{i=1}^3 s_i l_i$ and the matrix element of H_{SO} becomes[14]

$$\begin{aligned}
&\langle \gamma SLJM|H_{\mathrm{SO}}|\gamma' S'L'J'M'\rangle \\
&\quad = c_\zeta \zeta (-1)^{S'+L+J}\begin{Bmatrix} L & L' & 1 \\ S' & S & J \end{Bmatrix} \\
&\qquad \times \sum_{\overline{\gamma},S,L} \sqrt{(2S+1)(2S'+1)}\sqrt{(2L+1)(2L'+1)} \\
&\qquad \times \langle f^3\gamma SL\{|f^2\overline{SL}\rangle\langle f^3\gamma' S'L'\{|f^2\overline{SL}\rangle \\
&\qquad \times (-1)^{\overline{S}+s+S+\overline{L}+l+L}\begin{Bmatrix} s & s & 1 \\ S' & S & \overline{S} \end{Bmatrix} \\
&\qquad \times \begin{Bmatrix} l & l & 1 \\ L' & L & \overline{L} \end{Bmatrix} 3\sqrt{s(s+1)(2s+1)l(l+1)(2l+1)}.
\end{aligned} \tag{4}$$

The c parameters in Eqs. (2) and (4) will be determined below. The electric potential experienced by the Nd^{3+} ion will split the $Nd^{3+}(4f^3)$ free-ion energy levels into Stark levels

$$H_{\mathrm{CF}} = -\int dr'\ \frac{\rho(r')}{|r-r'|} = \sum_{t,p} A_{tp}^* \sum_i\ r_i^t C_{tp}(\hat{\mathbf{r}}_i), \tag{5}$$

where

$$A_{tp} = -\int dr'\ \frac{\rho(r')C_{tp}(\hat{\mathbf{r}}')}{r'^{t+1}}. \tag{6}$$

The matrix element of H_{CF} becomes[13]

$$\begin{aligned}
&\langle \gamma SLJM|H_{\mathrm{CF}}|\gamma' S'L'J'M'\rangle \\
&\quad = \sum_{t,p} A_{tp}^* \sum_i\ \langle r_i^t\rangle (-1)^{S+L'+t-M}\begin{pmatrix} J & t & J' \\ -M & p & M' \end{pmatrix} \\
&\qquad \times \sqrt{(2J+1)(2J'+1)}\begin{Bmatrix} L & L' & t \\ J' & J & S \end{Bmatrix} \\
&\qquad \times \sum_{S,L} \langle f^3\gamma SL\{|f^2\overline{SL}\rangle\langle f^3\gamma' S'L'\{|f^2\overline{SL}\rangle \\
&\qquad \times \sqrt{(2L+1)(2L'+1)}(-1)^{\overline{L}+l+L+t}\begin{Bmatrix} l & l & t \\ L' & L & \overline{L} \end{Bmatrix} \\
&\qquad \times (-1)^l(2l+1)\begin{pmatrix} l & t & l \\ 0 & 0 & 0 \end{pmatrix}\delta_{S'S}.
\end{aligned} \tag{7}$$

TABLE II. Values of MD potential parameters Eq. (26). The values are given in eV, Å, and eV Å.[6]

i	j	A_{ij}	ρ_{ij}	C_{ij}
Al	Al	0.0		0.0
Al	O	1460.3	0.299 12	0.0
Al	Y	0.0		0.0
Al	Nd	0.0		0.0
O	O	22 764.3	0.149	27.8
O	Y	1345.1	0.3491	0.0
O	Nd	1100.0	0.37	0.0
Y	Y	0.0		0.0
Y	Nd	0.0		0.0
Nd	Nd	0.0		0.0

Since we treat the Nd^{3+} environment as a sum of 2^n poles ($n=0,1,2,\ldots$), the integral (6) becomes a discrete sum, thus saving a great deal of computer time. A_{tp} is then given approximately by

$$\begin{aligned}
A_{tp} = \sum_j\ &[M_j^{(0)} r_j'^{-t-1} + D_j^{(1)}(t+1) r_j'^{-t-2} \\
&+ \tfrac{1}{2} Q_j^{(2)}(t+1)(t+2) r_j'^{-t-3}] C_{tp}(\Theta_j, \Phi_j),
\end{aligned} \tag{8}$$

where $M^{(0)}$, $D^{(1)}$, and $Q^{(2)}$ are the components of the monopole, dipole, and quadrupole moments, respectively, given by

$$D_{\hat{r}} = \hat{\mathbf{r}}^k \mathbf{D}_k, \tag{9}$$

$$Q_{\hat{r}} = \hat{\mathbf{r}}^k \hat{\mathbf{r}}^l \overleftrightarrow{\mathrm{Q}}_{kl}. \tag{10}$$

$\hat{\mathbf{r}}$ is the unit vector pointing from the rare-earth ion towards the neighboring ion under consideration; k and l are indices for the vector and tensor components, not to be confused with i or j, which label the ions:

$$M_i^{(0)} = q_i, \tag{11}$$

$$\mathbf{D}_i^{(1)} = -\alpha_i^{(1)} \sum_{j\neq i} \left\{ \boldsymbol{\nabla}\frac{1}{|\mathbf{r}_{ij}|} + \mathbf{D}_j^{(1)}\boldsymbol{\nabla}\boldsymbol{\nabla}\ \frac{1}{|\mathbf{r}_{ij}|} + \overleftrightarrow{\mathrm{Q}}_j^{(2)}\boldsymbol{\nabla}\boldsymbol{\nabla}\boldsymbol{\nabla}\ \frac{1}{|\mathbf{r}_{ij}|} \right\}, \tag{12}$$

$$\overleftrightarrow{\mathrm{Q}}_i^{(2)} = \alpha_i^{(2)} \sum_{j\neq i} \left\{ \boldsymbol{\nabla}\boldsymbol{\nabla}\ \frac{1}{|\mathbf{r}_{ij}|} + \mathbf{D}_j^{(1)}\boldsymbol{\nabla}\boldsymbol{\nabla}\boldsymbol{\nabla}\ \frac{1}{|\mathbf{r}_{ij}|} \right\}. \tag{13}$$

B. Oscillator strengths

The polarized oscillator strength for the electric-dipole transitions between eigenstates i and f is given by Ref. 15

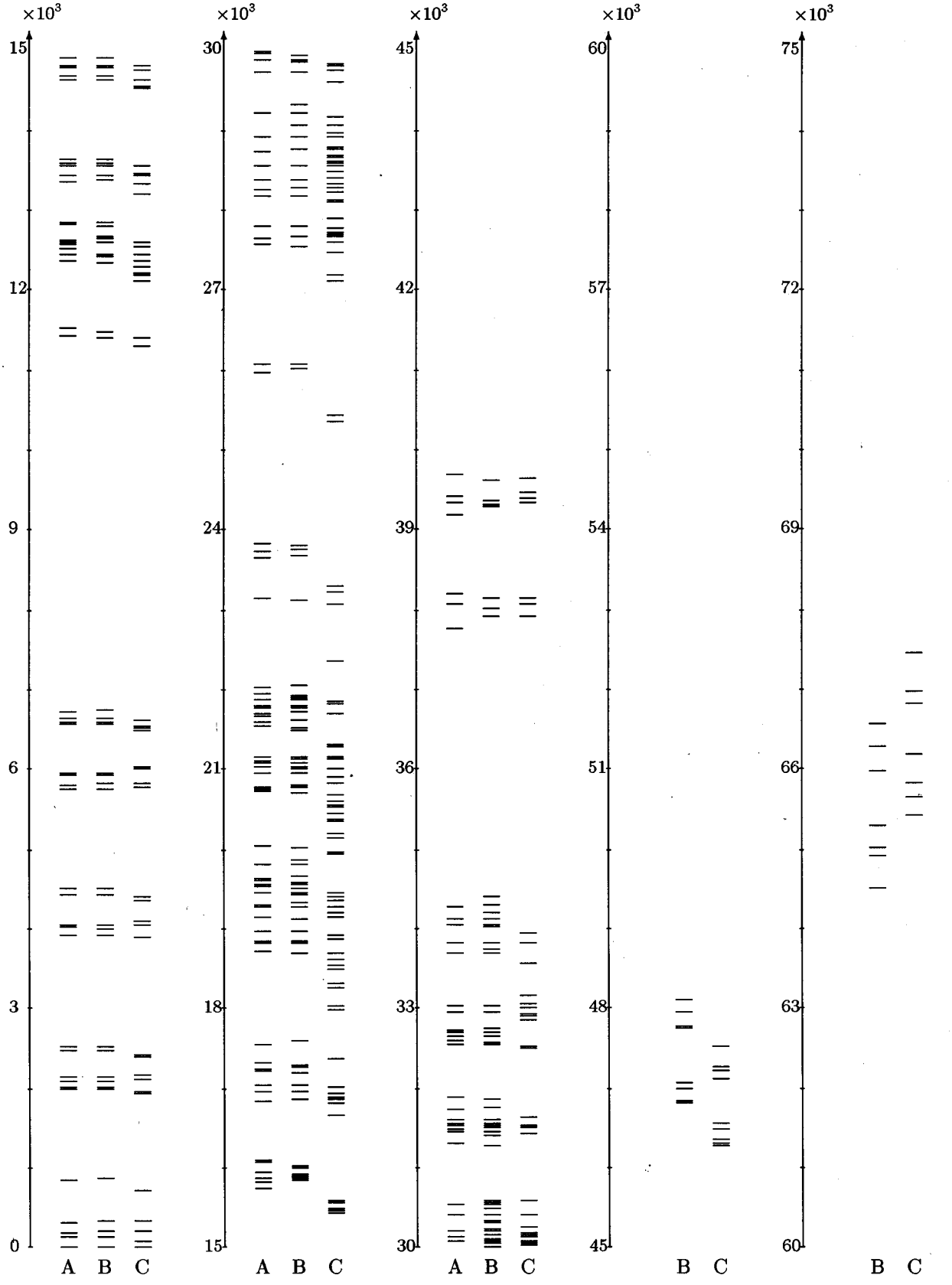

FIG. 1. Stark levels for the $Nd^{3+}(4f^3)$ electrons in cm^{-1}. Set *A*, experimental levels; set *B*, levels obtained from parameter fitting; set *C*, calculated Stark energies for A_{tp} parameters calculated as described in Sec. III A.

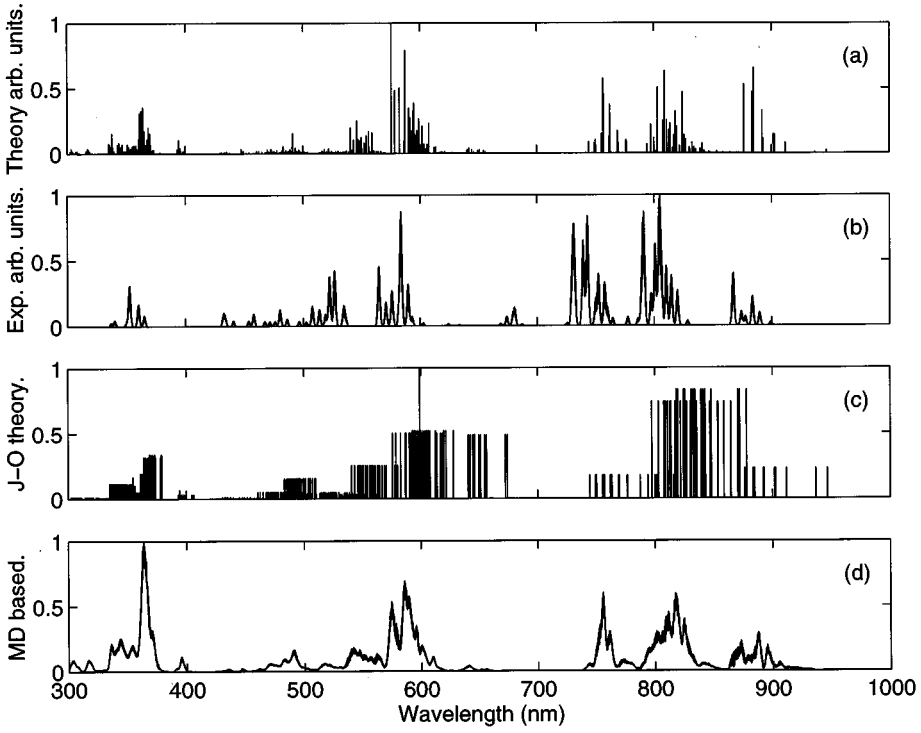

FIG. 2. (a) Calculated absorption intensities for all transitions from $^4I_{9/2}$ to $^4F_{3/2}$-$^2D_{5/2}$ at 300 K. The same eigenvectors have been used as those in set *C* of Fig. 1. (b) Experimental absorption spectrum of 1 wt. % Nd:YAG at 300 K. (c) Calculated absorption spectrum when Judd-Ofelt intensities have been assigned to each Stark transition. (d) Absorption spectrum summed over the 100 configurations obtained from a MD simulation at 300 K.

$$P_q(i,f)=\frac{1}{2}\chi\frac{8\pi^2 m\nu}{h}|\langle i|D_q^{(1)}|f\rangle|^2\frac{e^{-E_i/k_BT}}{\Sigma e^{-E_i/k_BT}}, \quad (14)$$

where

$$\langle i|D_q^{(1)}|f\rangle=\sum_{\lambda,t,p,i,f}(2\lambda+1)(-1)^{p+q}A_{tp}\begin{pmatrix}1 & \lambda & t\\ q & -p-q & p\end{pmatrix}\times a_i^* a_f(-1)^{J_i-M_i}\begin{pmatrix}J_i & \lambda & J_f\\ -M_i & p+q & M_f\end{pmatrix}\times\langle i\|U^{(\lambda)}\|f\rangle\Xi(t,\lambda) \quad (15)$$

and

$$\langle i\|U^{(\lambda)}\|f\rangle=\langle f^3[\gamma SLJ]\|U^{(\lambda)}\|f^3[\gamma' S'L'J']\rangle. \quad (16)$$

a_i^* and a_f are components of the initial and final eigenvectors. Equation (15) is a modified version of formula (3) of Ref. 16 and formula (7) of Ref. 15. The reduced matrix element of the unit tensor operator becomes[13]

$$\langle\gamma SLJ\|U^{(\lambda)}\|\gamma' S'L'J'\rangle=(-1)^{S+L'+\lambda-J}\sqrt{(2J+1)(2J'+1)}\times\begin{Bmatrix}L & L' & \lambda\\ J' & J & S\end{Bmatrix}\sum_{\overline{S,\ L}}\langle\gamma SL\{|\overline{SL}\rangle\times\langle\gamma' S'L'\{|\overline{SL}\rangle\sqrt{(2L+1)(2L'+1)}\times(-1)^{\overline{L}+l+L+\lambda}\begin{Bmatrix}l & l & \lambda\\ L' & L & \overline{L}\end{Bmatrix}. \quad (17)$$

$\Xi(t,\lambda)$ is evaluated using[17]

$$\Xi(t,\lambda)=2\sum_{n'l'}(2l+1)(2l'+1)(-1)^{l+l'}\begin{Bmatrix}1 & \lambda & t\\ l & l' & l\end{Bmatrix}\times\begin{pmatrix}l & 1 & l'\\ 0 & 0 & 0\end{pmatrix}\begin{pmatrix}l' & t & l\\ 0 & 0 & 0\end{pmatrix}\times\frac{\langle nl|r|n'l'\rangle\langle nl|r^t|n'l'\rangle}{\Delta E(n'l')}. \quad (18)$$

If the inhomogeneous dielectric mechanism[18,19] (IDM) is to be taken into account, the following matrix element (given by Ref. 20) must be evaluated, as well as the electric dipole matrix element:

$$\langle i|W^{\mathrm{IDM}}|f\rangle=\sum_{\lambda,t,p,i,f}\delta_{\lambda+1,t}\sqrt{(2t+1)(\lambda+1)(2\lambda+1)}\times(1-\sigma_\lambda)A_{tp}^{\mathrm{IDM}}(-1)^l(2l+1)\begin{pmatrix}l & \lambda & l\\ 0 & 0 & 0\end{pmatrix}\times(-1)^{p+q}\begin{pmatrix}1 & \lambda & \lambda+1\\ q & -p-q & p\end{pmatrix}a_i^* a_f\times(-1)^{J_i-M_i}\begin{pmatrix}J_i & \lambda & J_f\\ -M_i & p+q & M_f\end{pmatrix}\langle i\|U^{(\lambda)}\|f\rangle, \quad (19)$$

where A_{tp}^{IDM} is given by

$$A_{tp}^{\mathrm{IDM}}=\sum_j \alpha_j r_j'^{-t-1}C_{tp}(\Theta_j,\Phi_j). \quad (20)$$

Since YAG is optically isotropic, the oscillator strengths are calculated according to

TABLE III. Comparison of the intensity parameters Ω_λ (10^{-20} cm^2).

Ω_2	Ω_4	Ω_6	Ref.
0.51	1.97	6.98	this work
0.37	2.29	5.97	25[a]
0.2	2.7	5.0	26[a]
	8.9	8.9	22[b]
	8.0	9.4	22[b]
2.4	6.3	9.3	22[b]
0.79	7.1	9.3	22[b]

[a]Obtained from fits to room-temperature intensity data.
[b]Calculated with different intensity parametrizations and wave functions.

$$P(i,f)=\tfrac{1}{3}\sum_q P_q(i,f). \tag{21}$$

In standard Judd-Ofelt theory Ω_λ are the parameters of interest. Ω_λ is given by

$$\Omega_\lambda=(2\lambda+1)\sum_{t,p}\frac{|A_{tp}\Xi(t,\lambda)|^2}{2t+1}. \tag{22}$$

III. CALCULATIONS

A. Crystal field

It has been argued that more sophisticated models should be used when calculating the crystal-field parameters A_{tp}; see Refs. 7 and 8. However, our MD treatment has demonstrated large variations in these A_{tp} parameters. The use of such models would therefore seem to have only a minor effect by comparison. In the electrostatic model used here, the CF interaction with $Nd^{3+}(4f^3)$ electrons is defined by the A_{tp} parameters Eq. (8). The A_{tp} parameters must be corrected since the closed shells of the Nd^{3+} ion will not remain the same when exposed to the crystal field. This correction is taken into account by a redefinition of the CF parameters: $A_{tp}\rightarrow(1-\sigma_t)A_{tp}$, where σ_t are the shielding parameters;[6] see Table I. The summation (8) is performed until convergence of the A_{tp} parameters is achieved. The Nd^{3+} environment is expressed in a multipole expansion and the dipole and quadrupole polarizabilities used are obtained from *ab initio* calculations.[6,21] All dipole moments are calculated self-consistently, i.e., electrostatic equilibrium of charges and induced dipoles at each ion site is ensured. This is accomplished by rewriting Eq. (12) and solving the linear system of equations

$$\mathbf{D}^{(1)}=(\overleftrightarrow{1}+\alpha^{(1)}\overleftrightarrow{\mathrm{T}})^{-1}\alpha^{(1)}\mathbf{E}'. \tag{23}$$

$\alpha^{(1)}\mathbf{E}'_i$ is given by

$$-\alpha_i^{(1)}\sum_{j\neq i}\left\{\boldsymbol{\nabla}\frac{1}{|\mathbf{r}_{ij}|}+\overleftrightarrow{\mathrm{Q}}_j^{(2)}\boldsymbol{\nabla}\boldsymbol{\nabla}\boldsymbol{\nabla}\frac{1}{|\mathbf{r}_{ij}|}\right\} \tag{24}$$

and $\overleftrightarrow{\mathrm{T}}_{ij}$ is given by

$$\overleftrightarrow{\mathrm{T}}_{ij}=-\boldsymbol{\nabla}\boldsymbol{\nabla}\frac{1}{|\mathbf{r}_{ij}|}=\frac{1}{r_{ij}^3}\left(\overleftrightarrow{1}-3\frac{\mathbf{r}_{ij}\mathbf{r}_{ij}}{r_{ij}^2}\right). \tag{25}$$

In evaluating the effect on energy levels and oscillator strengths from the different electrostatic moments in the CF model, we have summed over all point charges within 70 Å of the Nd^{3+} ion and over all dipole and quadrupole moments within 8 Å of the Nd^{3+} ion in the summation (8). In most cases the convergence of the A_{1p} parameters is difficult to establish. However, in the case of Nd^{3+}:YAG the assumption of D_2 point-group site symmetry will force $A_{1p}=0$. This assumption will not be true once dynamics is considered. Therefore, setting $A_{1p}=0$ will only be an approximation.

B. Radial integrals

The radial integrals are evaluated using the radial wave functions obtained from Hartree-Fock-Dirac calculations[6] (see Table I for results and CI parameters). It is a well-known problem that the Slater integrals seem to be too large and the spin-orbit coupling constant too small to yield acceptable results. We have overcome this by introducing four CI parameters c_2, c_4, c_6, and c_ζ; see Eqs. (2) and (4).

C. Molecular dynamics

We can also study the temperature dependence of the spectrum, i.e., the sensitivity of various parameters to thermally induced fluctuations in the positions of neighboring ions, using MD. The standard ion-pair potential of the Born-Mayer-Huggins form has been used:

$$V_i=\sum_{i\neq j}q_iq_j/r_{ij}+A_{ij}\exp(-r_{ij}/\rho_{ij})-C_{ij}/r_{ij}^6. \tag{26}$$

The potential parameters fitted to reproduce the crystal structure and ion-ion distances are listed in Table II. The simulation box of $2\times2\times2$ unit cells contains 1280 atoms including two Nd^{3+} ions. The calculation procedure is repeated for each MD-generated Nd^{3+}-ion environment.

IV. RESULTS

The Stark levels for the $Nd^{3+}(4f^3)$ electrons are shown in Fig. 1. The first set of levels (A) is experimental,[22] the next (B) is obtained from fitting parameters to experiment.[22] Our calculated Stark splittings (set C) agree fairly well with experiment for most of the multiplets. The relative positions of the different multiples in set C agree fairly well with experiment, especially in the lower-energy region. One cannot expect good agreement with experiment in the higher-energy region because of the effects of the CI. This situation will improve when other configurations are included via second-order perturbation theory in the computation of the energy matrix.

The oscillator strengths for electric-dipole transitions within the $4f$ shell have been studied using a refinement of Judd-Ofelt theory. We have not considered the inhomogeneous dielectric mechanism (also referred to as the ligand polarization mechanism or as the dynamic coupling mechanism)[18,19] [see Eq. (19)] in the final results here; our study (when we have included the inhomogeneous dielectric

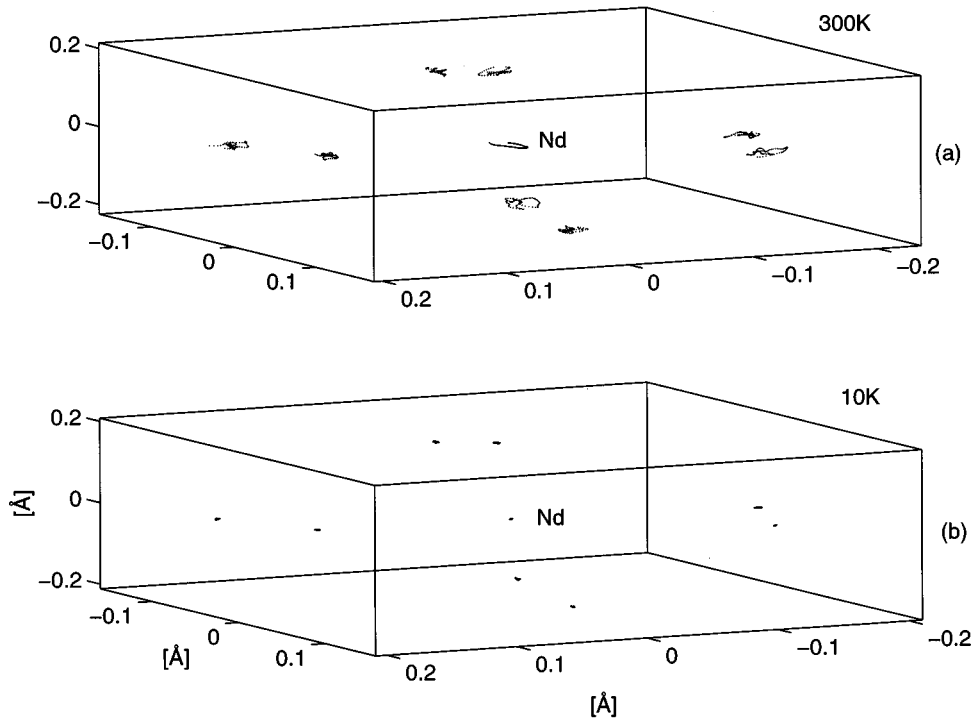

FIG. 3. Trajectories of a Nd^{3+} ion and its nearest neighbors at (a) 300 K and (b) 10 K. The picture consists of 100 snapshots.

mechanism) would suggest that this has only a negligible effect, at least in this case. The calculated electric-dipole polarized oscillator strengths vary significantly as a consequence of the large variations in the CF parameters resulting from our MD treatment. We feel it is important to fully investigate the simple model before including more ''sophisticated'' ones. Figure 2(a) shows the absorption intensities calculated for all the transitions from $^4I_{9/2}$ up to $^4F_{3/2}$-$^2D_{5/2}$ at 300 K. Eigenvectors belonging to the Stark energies of set C have been used to calculate the oscillator strengths. Figure 2(b) is an experimental absorption spectrum of 1 wt. % Nd:YAG at 300 K.[23] It is seen that qualitative agreement is obtained with experiment using an electrostatic model. The calculated oscillator strengths for the $^4I_{9/2} \rightarrow {}^4F_{3/2}$ transitions are too large, especially around 880 nm. From 750 to 850 nm and especially around 740 and 790 nm the oscillator strengths are too small. In the region 450–650 nm the difficulties are more pronounced, mainly because of less accurate eigenvectors. There are several reasons for this: (a) uncertainties in the reduced matrix elements because of errors in F^t and ζ, (b) uncertainties in the crystal-field parameters A_{tp} through neglect of of covalent effects and Ewald summations for $t=2,3$, and (c) nonlinear CI effects have not been treated.

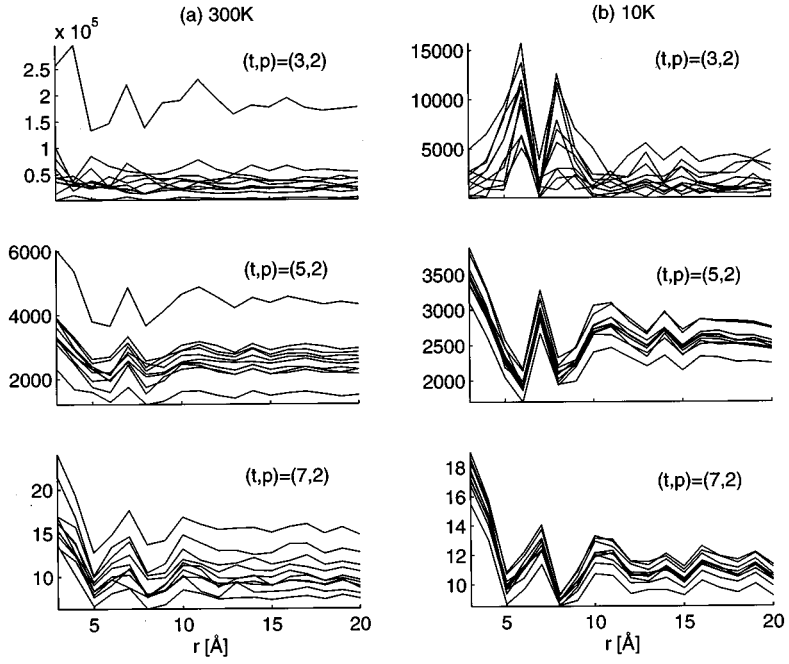

FIG. 4. Convergence plots for $|A_{tp}|^2$ (cm^{-2}) as a function of the radius of the summation sphere around the Nd^{3+} ion for ten typical Nd^{3+}-ion environments at (a) 300 K and (b) 10 K.

In standard Judd-Ofelt theory[17,24] the parameters of interest are the intensity parameters Ω_λ; see Eq. (22). Table III presents our derived Ω_λ values. The results are in good agreement with those obtained from fits to room-temperature intensity data. Discrepancies probably do not originate in our derived values but in the parameter fitting procedure, which has a number of weaknesses: (a) All parameters are not varied simultaneously, (b) energy levels can be incorrectly labeled, and (c) the different parameter sets that fulfill the minimization requirement in the fitting procedure are not unique. Figure 2(c) shows a calculated spectrum in which a Judd-Ofelt intensity has been assigned to the various transitions. Our calculated result shows better agreement with experiment than does the Judd-Ofelt–based result. This is expected since Judd[17] and Ofelt[24] summed away the MM' dependence and therefore lost spatial dependence. Judd and Ofelt also assumed equal occupation of the ground-state levels.

A MD simulation of Nd^{3+}:YAG has been performed to assess how the motion of the ions influences energies and oscillator strengths. MD generates a number of representative environments. We recalculate the crystal field and solve the eigenvalue problem for each of these environments. Figure 2(d) shows the spectra calculated for 100 different Nd^{3+} environments at 300 K. To compensate for this small number of environments, we have assigned a Gaussian distribution (with a full width at half maximum of 1.0 cm^{-1}) to each transition in the spectrum. The experimental agreement is seen to improve when the dynamical nature of the environment is accounted for. The overall profile of the spectrum is satisfactory, even though the oscillator strengths in the region below 400 nm are too large.

The trajectories for a Nd^{3+} ion and its nearest-neighbor environment during 30 fs are plotted in Fig. 3 at 300 and 10 K. Figure 4 shows convergence plots for $|A_{tp}|^2$ as a function of the distance r at 300 and 10 K for ten different representative environments. All ions within distance r from the Nd^{3+} ions are included in the summation (8). At 300 K, $|A_{tp}|^2$ values vary within $\pm 200\%$, $\pm 50\%$, and $\pm 40\%$ for $|A_{32}|^2$, $|A_{52}|^2$, and $|A_{72}|^2$, respectively. At 10 K, $|A_{tp}|^2$ values vary within $\pm 100\%$, $\pm 20\%$, and $\pm 10\%$ for $|A_{32}|^2$, $|A_{52}|^2$, and $|A_{72}|^2$, respectively. It is seen that $|A_{tp}|^2$ values vary greatly, even though they would seem to have converged for each individual environment. A MD simulation is indeed motivated, even at low temperatures, especially when calculating oscillator strengths since these depend on $|A_{tp}|^2$ and therefore do not average out around, for example, an inversion center.

V. CONCLUSION

Qualitative agreement is obtained between experimental and calculated Stark level splittings and oscillator strengths using only four experimentally deduced parameters. Agreement should not be expected for the relative positions of the different multiplets since the effects of the CI are not treated rigorously. Inclusion of the CI will improve the agreement and allow us to remove the four parameters that correct the Slater integrals and the spin-orbit constant. MD simulation is also clearly needed to generate different representative environments for the Nd^{3+} ion since energies and particularly oscillator strengths are highly sensitive to motion of the neighboring ions.

ACKNOWLEDGMENTS

This work has been supported by grants from The Swedish Natural Science Research Council and by the U.S. Office of Naval Research.

*Present address: Department of Physics and Mathematics, Mid Sweden University, S-851 70 Sundsvall, Sweden.

[1] G. Racah, Phys. Rev. **61**, 186 (1942).
[2] G. Racah, Phys. Rev. **62**, 438 (1942).
[3] G. Racah, Phys. Rev. **63**, 367 (1943).
[4] G. Racah, Phys. Rev. **76**, 1352 (1949).
[5] K. Rajnak and B. G. Wybourne, Phys. Rev. **132**, 280 (1963).
[6] S. Edvardsson and M. Klintenberg (unpublished).
[7] D. Garcia and M. Faucher, *Handbook on the Physics and Chemistry of Rare Earths* (Elsevier, New York, 1995), Vol. 21, p. 263.
[8] D. J. Newman and B. Ng, Rep. Prog. Phys. **52**, 699 (1989).
[9] B. Ng and D. J. Newman, J. Chem. Phys. **83**, 1758 (1985).
[10] B. Ng and D. J. Newman, J. Chem. Phys. **87**, 7096 (1987).
[11] B. Ng and D. J. Newman, J. Chem. Phys. **87**, 7110 (1987).
[12] M. F. Reid and B. Ng, Mol. Phys. **67**, 407 (1989).
[13] B. R. Judd, Proc. R. Soc. London Ser. A **250**, 562 (1959).
[14] B. R. Judd, *Operator Techniques in Atomic Spectroscopy* (McGraw-Hill, New York, 1963).
[15] S. Edvardsson, M. Klintenberg, and J. O. Thomas, Phys. Rev. B **54**, 17 476 (1996).
[16] P. Porcher and P. Caro, J. Lumin. **21**, 207 (1980).
[17] B. R. Judd, Phys. Rev. **127**, 750 (1962).
[18] C. K. Jørgensen and B. R. Judd, Mol. Phys. **8**, 281 (1964).
[19] B. R. Judd, J. Chem. Phys. **70**, 4830 (1979).
[20] O. L. Malta, S. J. L. Ribeiro, M. Faucher, and P. Porcher, J. Phys. Chem. Solids **52**, 587 (1991).
[21] P. C. Schmidt, A. Weiss, and T. P. Das, Phys. Rev. B **19**, 5525 (1979).
[22] G. W. Burdick, C. K. Jayasankar, F. S. Richardson, and M. F. Reid. Phys. Rev. B **50**, 16 309 (1994).
[23] M. A. Kramer and R. W. Boyd, Phys. Rev. B **23**, 986 (1981).
[24] G. S. Ofelt, J. Chem. Phys. **37**, 511 (1962).
[25] A. A. Kaminskii and L. Li, Phys. Status Solidi A **26**, K21 (1974).
[26] W. F. Krupke, IEEE J. Quantum Electron. **7**, 153 (1971).